

Original Article

ST2-104 attenuates neuronal injuries in A β_{25-35} -induced AD rats by inhibiting CRMP2-NMDAR2B signaling pathways

Yingshi Ji¹, Panpan Meng¹, Yang Hu¹, Rajesh Khanna², Yuqing Zhang¹, Qi Li¹, Jinghong Ren¹, Li Sun³

¹Department of Pharmacology, College of Basic Medical Sciences, Jilin University, Changchun 130021, Jilin, P. R. China; ²Department of Pharmacology, College of Medicine, University of Arizona, Tucson, Arizona 85724, USA; ³Department of Neurology and Neuroscience Center, The First Hospital, Jilin University, Changchun 130021, Jilin, P. R. China

Received August 21, 2018; Accepted October 8, 2018; Epub March 15, 2019; Published March 30, 2019

Abstract: Collapsin response mediator protein 2 (CRMP2), traditionally regarded as an axon/dendrite growth and guidance protein, plays an important role in the regulation of both post- and pre-synaptic Ca²⁺ channels, such as N-methyl-d-aspartate receptors (NMDARs). The Ca²⁺ channel-binding domain 3 (CBD3) peptide derived from CRMP2 has recently emerged as a Ca²⁺ channel blocker, suppressing neuropathic pain in a spared nerve injury (SNI) model when linked to the transduction domain of HIV TAT protein and reduced neuronal death in a middle cerebral artery occlusion model and a traumatic brain injury (TBI) model. The present study aimed to examine the neuroprotective effects and biochemical mechanisms of ST2-104 (a non-arginine-conjugated CBD3 peptide) in an A β_{25-35} -induced Alzheimer's disease (AD) rat model. This study demonstrated that CRMP2 and NMDARs subunit NMDAR2B form a direct biochemical complex, which regulates NMDAR activity in a rat model. ST2-104 peptide given via tail vein injections significantly reduced spatial learning and memory impairment. ST2-104 relieved neuronal injuries by suppressing expression of NMDAR2B and p-CRMP2 and increasing expression of CRMP2 in the hippocampus. Remarkably, ST2-104 attenuated levels of intracellular Ca²⁺ by disrupting the interaction between p-CRMP2 and NMDAR2B. Taken together, these findings support ST2-104 as a novel neuroprotective agent, potentially representing a novel direction for a therapeutic targeting channel in AD.

Keywords: Alzheimer's disease, A β_{25-35} , CRMP2, NMDAR2B, ST2-104, neuroprotection

Introduction

Alzheimer's disease (AD) is an age-related progressive neurodegenerative disorder, characterized by learning, spatial memory, and cognitive dysfunction [1]. Main pathological changes include a decrease in synapses and neurons, amyloid beta protein deposition, and neurofibrillary tangles in the cortex, especially in the hippocampus [2, 3]. Current treatments cannot effectively improve the manifestation and block the progression of the disease [4]. Therefore, creating a new therapeutic strategy is necessary for treatment of AD.

Glutamate receptors, in particular NMDARs, are widely distributed in the hippocampus [5]. NMDARs can mediate many functions, including physiological functions and pathological damage [6]. A growing body of literature has

shown that A β deposition can act directly on NMDARs, leading to continuous NMDAR activation and eventual neural degeneration [7, 8]. This is because the promotion of Ca²⁺ influx through NMDARs may lead to intracellular Ca²⁺ overload in the postsynaptic neuron, the inhibition of synaptic function, long term potentiation (LTP) exception, and cell death [9-11]. Therefore, NMDAR dysfunction plays a crucial role in the pathogenesis of AD. Targeting NMDARs is a promising strategy for AD. It was confirmed that the activation of NMDARs can be regulated by various factors [12]. CRMP2, an abundant brain-enriched protein, is a novel binding partner of NMDARs, which is highly phosphorylated by CDK5 and GSK3 β in AD brains [13, 14]. It was shown that the phosphorylation of CRMP2 can strengthen the interaction between CRMP2 and NMDARs, causing excessive NMDARs activation, whereas block-

ing the combination of CRMP2 and NMDARs or knocking out CRMP2 could protect neurons from cerebral ischaemia and brain trauma [15, 16]. In summary, the present study hypothesizes that CRMP2/NMDAR interactions may play an important role in AD and that the modulation of NMDARs by CRMP2 may have a protective effect on neurons.

CRMP2-derived peptide (namely ST2-104) is a non-arginine (R9)-conjugated CBD3 peptide. Its molecular weight is 3056.6 g/mol. It has been confirmed that ST2-104 is a neuroprotective peptide in glutamate-mediated neurotoxicity by blocking the combination of CRMP2 and NMDARs in brain trauma and cerebral haemorrhages. It has been shown that ST2-104 exhibits a suppressive effect in rats with peripheral neuropathy, whereas the effects of ST2-104 on AD have not been fully certified. Further investigation is urgently needed.

It was hypothesized that $A\beta_{25-35}$ enhances levels of p-CRMP2, which intensively interacts with NMDARs leading to the hyperactivation of NMDARs. Hyperactive NMDARs lead to an excessive influx of Ca^{2+} ions that, in turn, lead to the disorder of intracellular calcium homeostasis and cell death following excitotoxicity.

Based on these results, this study proposed a model that explains the roles of CRMP2 in the regulation of NMDARs and elucidates the feasible mechanisms of ST2-104 neuroprotective effects.

Materials and methods

Materials

$A\beta_{25-35}$ was purchased from Sigma-Aldrich (A4559; St. Louis, USA). ST2-104 was synthesised by Yaoqiang Biological Company (Jiangsu, China). Memantine hydrochloride was obtained from H. Lundbeck A/S (Denmark). Primary antibodies against GAPDH (ab37168), NMDAR2B (ab93610), NMDAR1 (ab52177), CRMP2 (ab129082), and pCRMP2 (ab193226) were purchased from Abcam (Cambridge, MA, USA). Secondary antibodies, NP-40 lysis buffer, BCA protein assay kit, DAB chromogen kit, protein A/G agarose beads, Fluo-3 AM, and D-Hank's solution were purchased from the Beyotime Institute of Biotechnology (Shanghai, China). PVDF membranes and western ECL substrate were purchased from Bio-Rad (USA). RPMI-1640 medium was purchased from Gibco

(Shanghai, China). Foetal bovine serum was purchased from Biological Industries (04-001-1ACS; Israel).

Animals

Male Wistar rats (280-310 g) were purchased from the Animal Experimental Center of Jilin University. The rats were controlled in an animal house with a temperature of $22 \pm 2^\circ\text{C}$ and humidity of $60\% \pm 5\%$, with a 12-hour light/dark cycle. Rats were provided with free access to food and water. Rats were randomly separated into five groups ($n=10$ in each group): Con group, Model group ($A\beta_{25-35}$ 15 nmol), ST2-104 (ST2-104 3 or 15 mg/kg + $A\beta_{25-35}$ 15 nmol) groups, and Memantine (memantine hydrochloride 3 mg/kg + $A\beta_{25-35}$ 15 nmol) group.

Cell culture and treatment

Human neuroblastoma cell line SH-SY5Y was purchased from KeyGen Biotech (Jiangsu, China). These cells were verified to be of human origin by hybridization of human DNA probes to SH-SY5Y genomic DNAs and control DNAs on nylon membrane. Cells were cultured in RPMI-1640 medium supplemented with 10% foetal bovine serum in a saturating humidified incubator with 5% CO_2 at 37°C . To study the levels of intracellular free Ca^{2+} , cells were seeded into 6-well plates at a density of 2×10^5 cells/mL. Upon reaching 70% confluence, cells were treated with $3 \mu\text{M}$ $A\beta_{25-35}$ for 24 hours to induce excitatory damage. Cells were pre-treated with doses of ST2-104 (1, 3, or 10 μM) for 0.5 hours, then $3 \mu\text{M}$ $A\beta_{25-35}$ was added to the medium for 24 hours of co-incubation.

$A\beta$ aggregation

$A\beta_{25-35}$ was dissolved in 1% acetic acid and diluted in PBS to a final concentration of 2 $\mu\text{g}/\mu\text{l}$ and 1 mM, then incubated at 37°C for 7 days to obtain aggregated $A\beta_{25-35}$. Aggregated $A\beta_{25-35}$ was sub-packaged with an EP tube and stored at -20°C for future use.

Surgery procedure and treatment

A rat model of AD was established using a single dose of $A\beta_{25-35}$ via intracerebroventricular injections. Briefly, rats were anesthetized with 10% chloral hydrate (350 mg/kg) by intraperitoneal injections. Rats were then fixed onto a stereotaxic apparatus (Ward life technology co., LTD). The skull was exposed and a bregma

Neuroprotection of ST2-104 in $A\beta_{25-35}$ -induced AD

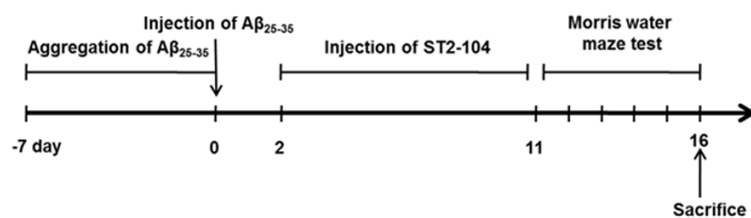


Figure 1. Experimental schedule and time-line of drug treatment.

was located. The injection coordinates were 1.8 mm lateral, 1.08 mm posterior, and 3.8 mm ventral to the bregma. A hole (diameter 1.0 mm) was drilled into the skull to expose the lateral ventricles. Rats in the model group and treatment group received injections in both lateral ventricles using a micro-syringe. The injection volume of $A\beta_{25-35}$ for each rat was 8 μ L (15 nmol). After the injection, the needle was left for 10 minutes and removed slowly. Rats in the sham group received an equivalent volume of normal saline. During surgery, the rectal temperature of the rats was maintained at 37°C. After surgery, the incision was sutured. The animals were returned to their cages and kept warm until they recovered consciousness.

Rats in the drug intervention groups were intravenously administered ST2-104 (3 or 15 mg/kg) and memantine hydrochloride (3 mg/kg) from day 2 to day 11. The Con group and Model group were administered saline in parallel. All animal procedures were approved by the Ethics Committee for the Use of Experimental Animals of Jilin University. The experimental schedule is shown in **Figure 1**.

Morris water maze test

Morris water maze tests were performed from days 12 to 16. A circular black painted pool (150 cm in diameter, 30 cm in depth) was randomly divided into four quadrants. The pool was filled with water maintained at 22°C \pm 0.5°C. An invisible escape platform (10 cm in diameter) was submerged 1 cm under the water surface in one quadrant. During the process of training, the platform remained in a fixed location. Rats were trained for 5 consecutive days, five trials per day. During each trial, rats were placed into the water from random starting points facing the pool wall until they found a hidden platform. Escape latency, the time needed to climb up the platform, was measured. If the rat could not find the platform within 120 seconds, it was guided to the plat-

form and escape latency was recorded as 120 seconds. On day 16, rats were subjected to a space probe test. For this test, the platform was removed and the rats were permitted to search for the platform for 120 seconds. During the Morris water maze tests, behaviour was monitored with a

camera positioned over the pool. The number of crossings over the original platform quadrant and the time spent in the target quadrant were measured and analyzed using the Super Maze Morris software (Shanghai Softmaze Information Technology Co. Ltd., Shanghai, China). Behaviour tests were performed by 2 investigators blinded to the experimental groups.

Brain tissue preparation

After the Morris water maze test, all rats were sacrificed by an overdose of 10% chloral hydrate (600 mg/kg). This was the primary method of euthanasia employed. Their brains were removed immediately. The hippocampi of the rats were dissected, rapidly frozen in liquid nitrogen, and stored at -80°C until the assay. For histological and immunohistochemical staining, animals were perfused with 0.9% normal saline (100 mL), followed by 4% paraformaldehyde (pH 7.35, 350 mL). Brains were then removed and further fixed with 4% paraformaldehyde at 4°C until slicing.

Histological and immunohistochemical staining

Brain tissues were embedded with paraffin and cut into 5- μ m serial coronal sections. For histology, sections containing the hippocampus were hydrated and stained with haematoxylin and eosin solution. They were then dehydrated and finally cover slipped. For immunohistochemistry, sections were treated with 3% H_2O_2 for 5 minutes and blocked with 5% normal goat serum at room temperature for 30 minutes. Sections were then incubated with primary antibodies [p-CRMP2 (ab193226), CRMP2 (ab129082), NMDAR1 (ab52177), NMDAR2B (ab93610), 1:500; Abcam] overnight at 4°C, washed with PBS, and further incubated with biotinylated anti-mouse anti-rabbit secondary antibodies (1:2,000; Beyotime) for 1 hour at room temperature. After washing with TBS

three times, sections were visualized using a DAB chromogen kit (Beyotime, Shanghai, China) for 10 minutes at room temperature. The sections were observed under a light microscope and 5 random fields in each section were analyzed using Image Pro Plus 6.0 software. For negative controls, primary antibodies were replaced by PBS.

Western blot analysis

Brain tissues from rat hippocampi were homogenized with lysis buffer (Beyotime, Shanghai, China). Protein concentrations were determined using a BCA protein assay kit (Beyotime, Shanghai, China). All samples were diluted in loading buffer (Beyotime, Shanghai, China). Thirty micrograms of protein were run on 10% SDS-PAGE and subsequently transferred onto PVDF membranes (Bio-Rad). The membranes were incubated with 5% non-fat milk in TBST (10 mM Tris-HCl, 150 mM NaCl, and 0.1% Tween-20 (v/v)) for 2 hours at room temperature, then incubated overnight at 4°C with the primary antibodies [GAPDH (ab37168), p-CRMP2 (ab193226), CRMP2 (ab129082), NMDAR1 (ab52177), NMDAR2B (ab93610), 1:1,000; Abcam]. Membranes were incubated at room temperature for 2 hours with the secondary antibody (anti-rabbit or anti-mouse IgG, 1:1,000; Beyotime). Protein bands were visualized with the ECL reagent using the GENIE Imaging system. Intensities of the protein bands were analyzed using Quantity One software.

Co-immunoprecipitation analysis

Rat hippocampal tissues were homogenized in NP-40 lysis buffer (Beyotime, Shanghai, China). Protein was quantified with a BCA kit. Two micrograms of anti-NMDAR2B (ab93610; Abcam) primary antibody was added to the lysate (500 μ g) and rotated at 4°C for 2 hours. Protein A/G agarose beads were added, then the mixture was rotated overnight at 4°C. The beads were washed with PBS five times and then resuspended in loading buffer and boiled for 5 minutes. After centrifugation for 5 minutes, the supernatant was processed by immunoblotting using an anti-p-CRMP2 (ab93610; 1:1,000; Abcam) antibody and proper second antibody.

Intracellular free Ca^{2+} detection

Intracellular free Ca^{2+} was detected using fluorescent dye Fluo-3 AM (Beyotime, Shanghai,

China). It can easily permeate cells but not bind Ca^{2+} , then be readily resolved into Fluo-3 by intracellular esterase. Having combined with Ca^{2+} , the Fluo-3 emits strong fluorescence at an excitation wavelength of 488 nm. SH-SY5Y cells in 6-well plates were loaded with Fluo-3 AM (5 μ M) in D-Hank's balanced salt solution in incubator for 30 minutes. Treated cells were collected and washed three times with D-Hank's balanced salt solution. Resulting fluorescence was detected by flow cytometer (Bio-Rad) with an emission wavelength of 525 nm and an excitation wavelength of 488 nm.

Statistical analysis

Experimental data are expressed as the mean \pm S.E. Statistical analyses were performed by one-way analysis of variance (ANOVA) and Tukey's statistics using Prism 5. Data are considered statistically significant when $P < 0.05$.

Results

Protective effects of ST2-104 against $A\beta_{25-35}$ -induced spatial learning and memory impairment in rats

The effects of ST2-104 (3 or 15 mg/kg, iv.) on spatial learning and memory in $A\beta_{25-35}$ -induced rats were investigated using the Morris water maze test. Escape latency reductions, day by day, reflected learning with regards to long-term memory. Compared with the Control group, escape latencies were significantly increased in the Model group, ($P < 0.01$). The increased escape latency by $A\beta_{25-35}$ was significantly decreased in the ST2-104 (3 or 15 mg/kg) plus $A\beta_{25-35}$ group, compared to the Model group ($P < 0.01$, **Figure 2A**). In probe trials, a significant decrease in the number of rats crossing over the original platform was recorded in the $A\beta_{25-35}$ oligomer-induced rats, compared with the Control rats ($P < 0.01$), and recovered by treatment with ST2-104 (3 or 15 mg/kg) ($P < 0.05$, $P < 0.01$, **Figure 2C**). In addition, ST2-104-treated rats spent significantly more time in the target quadrant than the Model rats ($P < 0.01$, **Figure 2B**). These data demonstrate that treatment with aggregated $A\beta_{25-35}$ resulted in the impairment of spatial learning and memory, while treatment with ST2-104 (3 or 15 mg/kg) significantly improved $A\beta_{25-35}$ -induced memory loss. Memantine hydrochloride is an antagonist of NMDAR used as positive control in the inves-

Neuroprotection of ST2-104 in $A\beta_{25-35}$ -induced AD

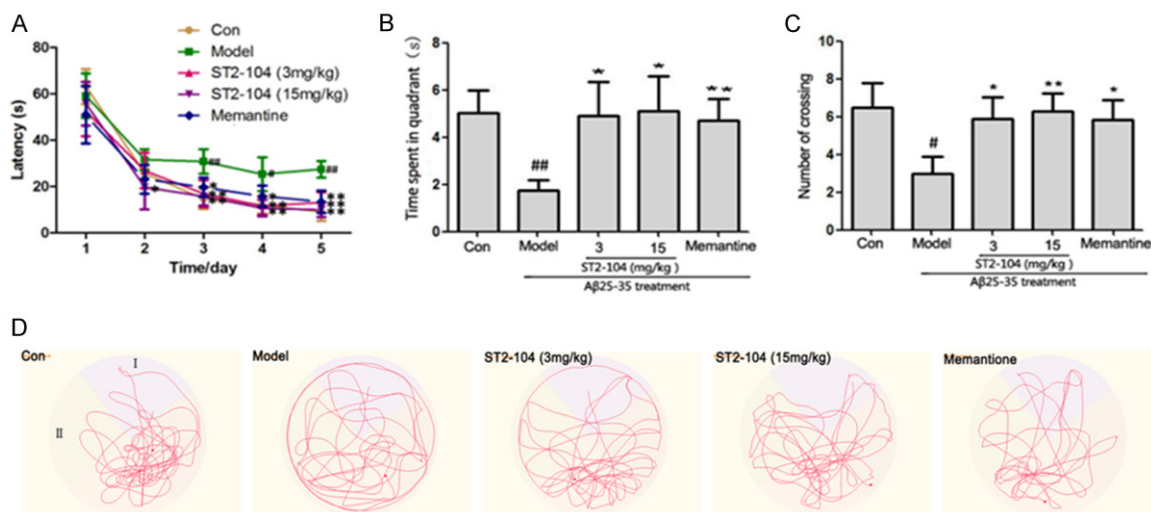


Figure 2. The effects of ST2-104 on $A\beta_{25-35}$ -induced cognitive impairment. A. Quantitative analysis of latency period. B. Time spent in the target quadrant. C. Number of crossings over original platform. D. Localization trial pathway. Data are shown as mean \pm standard deviation from at least three independent experiments. * $P < 0.05$ and ** $P < 0.01$ vs. control group; # $P < 0.05$ and ## $P < 0.01$ vs. Model group. $n = 10$.

tigation. The effectiveness of ST2-104 was in accord with that of memantine hydrochloride at 3 mg/kg.

ST2-104 inhibited histopathological damage of the hippocampus in $A\beta_{25-35}$ -induced rats

H&E staining was conducted to evaluate neuronal injuries in $A\beta_{25-35}$ -induced rats. In contrast to the Control group, obvious histopathological damage was observed in the hippocampi from the Model group. Neuronal loss was found in the CA1 region and the pyramidal layered structure was broken. Hippocampus CA1 areas in the Model group appeared to have a loose arrangement of neurons. These abnormalities were attenuated by ST2-104 treatment (Figure 3A). The number of normal neurons in the CA1 region of the hippocampus was counted under a light microscope. It was found that the average number of normal pyramidal cells in the Model group was lower than the Control group. Moreover, ST2-104 (3 or 15 mg/kg, iv.) treatment significantly increased the number of normal pyramidal cells ($P < 0.01$, Figure 3B).

ST2-104 suppressed NMDAR2B in the hippocampus of $A\beta_{25-35}$ -induced rats

To investigate the neuroprotective mechanisms of ST2-104, NMDAR1/NMDAR2B protein expression in hippocampal CA1 neurons was tested by immunohistochemistry and Western blotting. Regarding immunohistochemistry, as shown in Figure 4, the optical density of NM-

DAR2B was significantly higher in the Model group than in the control group, indicating that the number of NMDAR2B-positive neurons was increased. Compared with the Model group, treatment with ST2-104 (15 mg/kg) notably decreased the number of NMDAR2B-positive cells in the hippocampus ($P < 0.01$, Figure 4B, 4D). In contrast, NMDAR1-positive neurons were not significantly increased in the Model group and ST2-104 treatment did not show a significant alteration in NMDAR1-positive neurons (Figure 4A, 4C, $P > 0.05$). As shown in Figure 4F, the relative density of NMDAR2B of model rats was significantly increased. ST2-104 inhibited the effects of $A\beta_{25-35}$ on levels of NMDAR2B ($P < 0.05$). In addition, the relative density of NMDAR1 was not significantly increased in the Model group and ST2-104 treatment did not show a significant alteration in NMDAR1-positive neurons (Figure 4E). Results suggest that neuroprotection of ST2-104 was partly mediated by the downregulation of the NMDAR2B receptor, but not the NMDAR1 receptor, in the hippocampi of $A\beta_{25-35}$ -induced rats.

ST2-104 increased expression of CRMP2 and reduced expression of p-CRMP2 in the hippocampi of $A\beta_{25-35}$ -induced rats

To investigate whether ST2-104 protects neurons against $A\beta_{25-35}$ -induced injuries by enhancing CRMP2 and reducing p-CRMP2, this study measured expression of p-CRMP2/CRMP2 protein in the hippocampus. As seen in Figure 5A

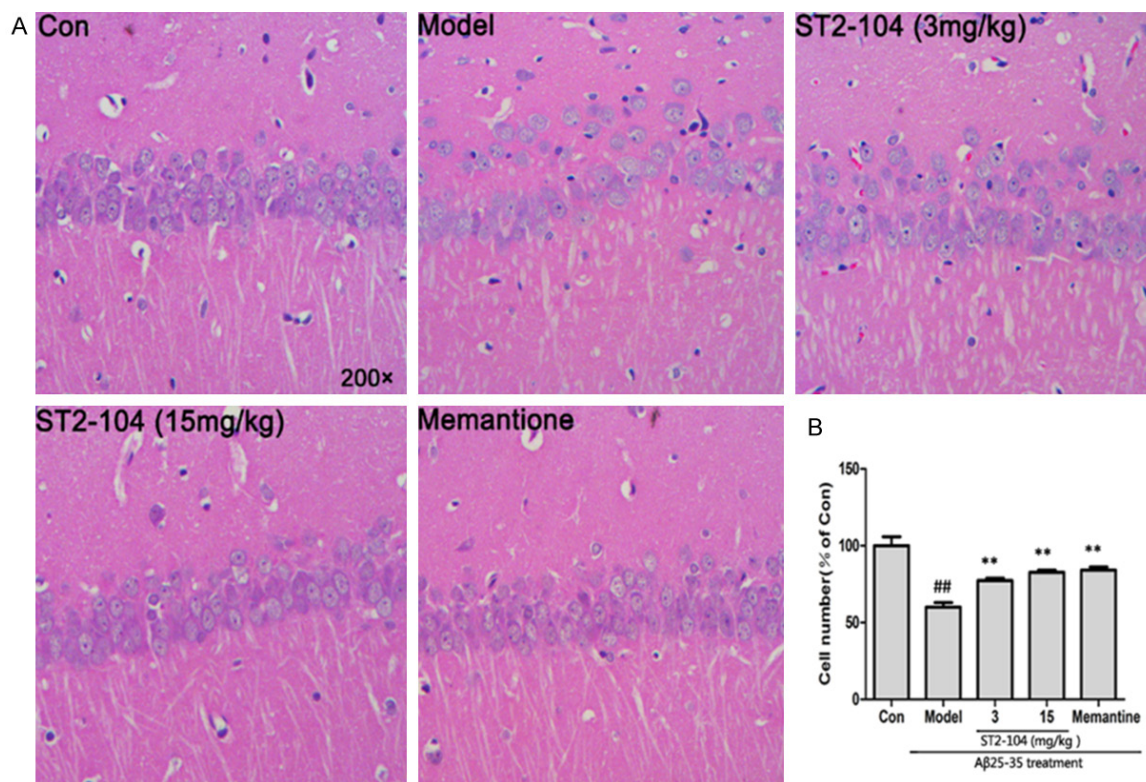


Figure 3. ST2-104 increased the number of normal neurons in the hippocampus of $A\beta_{25-35}$ -induced rats. A. HE staining. B. The number of normal neurons in the CA1 region of hippocampus was counted under a light microscope (magnification 200 \times). Data are shown as the mean \pm standard deviation. ## $P < 0.01$ vs. Con; ** $P < 0.01$ vs. Model. $n = 10$.

and **5F**, CRMP2 appeared to be localized in both the plasma membrane and cytoplasm, while neurons positive for CRMP2 were significantly decreased in the Model group, compared to the control group ($P < 0.01$). This pattern of expression was significantly reversed by ST2-104 treatment relative to the Model group ($P < 0.05$). As shown in **Figure 5B** and **5G**, both Western blot and immunochemical staining showed that pCRMP2 was attenuated after being induced and upregulated by ST2-104 treatment.

ST2-104 disrupted the interaction of p-CRMP2/NMDAR2B in the hippocampus of $A\beta_{25-35}$ -induced rats

To confirm the interactions of p-CRMP2/NMDAR2B, immunoprecipitation analysis was performed. As shown in **Figure 6**, an interaction between p-CRMP2 and NMDAR2B was notably strengthened in $A\beta_{25-35}$ -induced rats. ST2-104 disrupted the p-CRMP2-NMDAR2B complex. Inhibition of NMDAR2B activity by TAT-CBD3 suggests a direct interaction between p-CRMP2 and NMDAR2B. These experiments were

focused on the interaction of p-CRMP2 with NMDAR2B because this type of NMDAR is predominantly involved in excitotoxicity. It is possible that p-CRMP2 upregulates NMDAR activity by binding to the NMDAR2B subunit and that TAT-CBD3-mediated dissociation of p-CRMP2 from NMDAR2B leads to diminution of NMDAR activity.

ST2-104 suppressed levels of intracellular free Ca^{2+} concentrations in $A\beta_{25-35}$ -induced SH-SY5Y cells

Dysregulation in intracellular free Ca^{2+} has been recognized as one of the factors for cell injury and death [17, 18]. With this in mind, Fluo-3 AM was used to detect the effects of ST2-104 on intracellular free Ca^{2+} in SH-SY5Y cells. As shown in **Figure 7**, there were dramatically elevated Ca^{2+} levels in SH-SY5Y cells treated with $A\beta_{25-35}$ compared with control cells or cells treated with ST2-104. With increasing ST2-104 concentrations, the decrease in Ca^{2+} levels were more evident. Results indicate that the neuroprotective effects of ST2-104 were related to intracellular Ca^{2+} homeostasis.

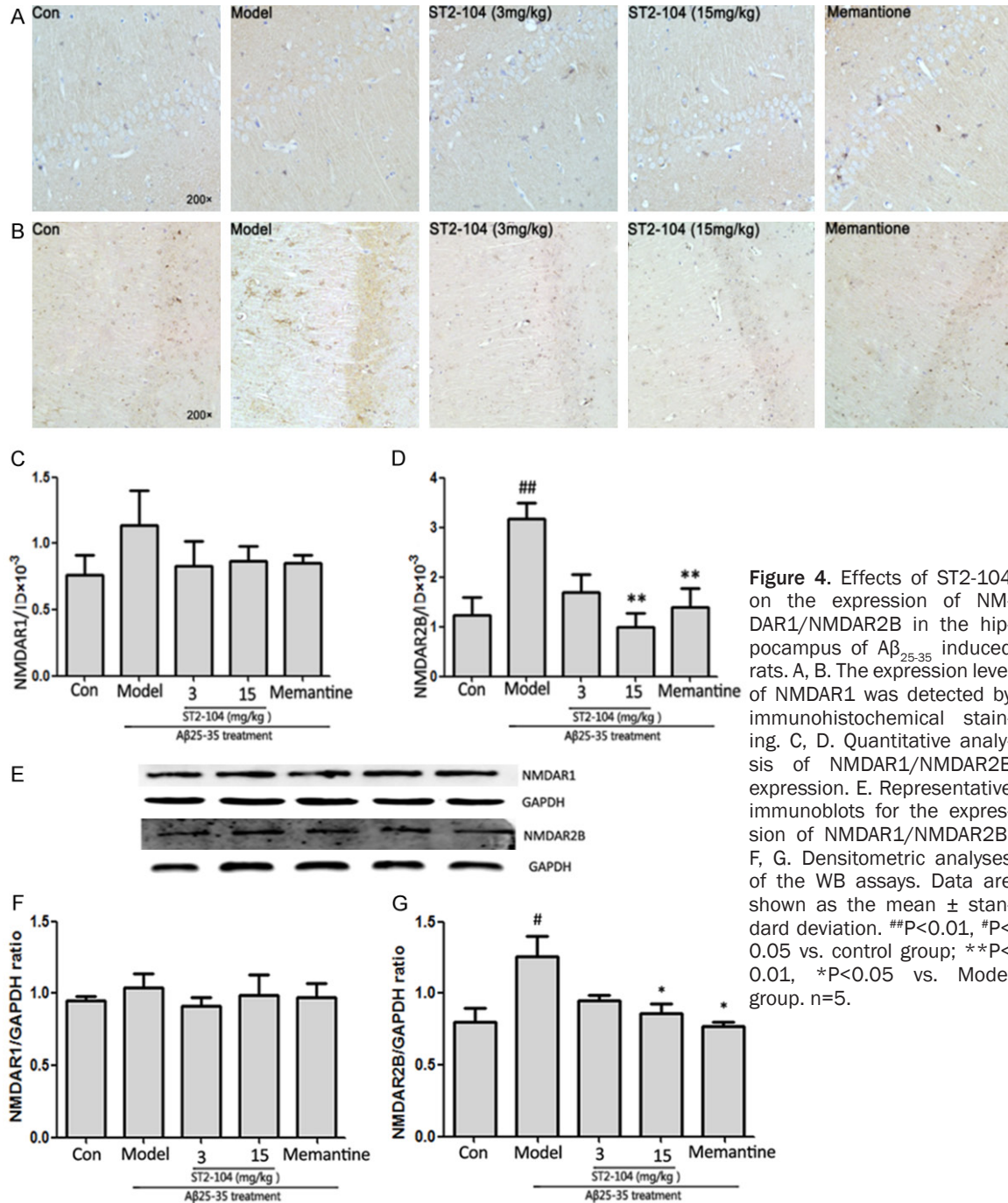


Figure 4. Effects of ST2-104 on the expression of NMDAR1/NMDAR2B in the hippocampus of $A\beta_{25-35}$ induced rats. A, B. The expression level of NMDAR1 was detected by immunohistochemical staining. C, D. Quantitative analysis of NMDAR1/NMDAR2B expression. E. Representative immunoblots for the expression of NMDAR1/NMDAR2B. F, G. Densitometric analyses of the WB assays. Data are shown as the mean \pm standard deviation. ^{##} $P < 0.01$, [#] $P < 0.05$ vs. control group; ^{**} $P < 0.01$, ^{*} $P < 0.05$ vs. Model group. $n = 5$.

Discussion

CRMP2 is an intracellular phosphoprotein, known as a neurite extension-promoting neuronal molecule, implicated in the advance of the neuronal growth cone [19-21]. CRMP-2 contributes to axon formation by binding to tubulin heterodimers and promoting the assembly of microtubules with axonal growth and differentiation [22]. CRMP2 has been reported to be

implicated in many neurological diseases, including AD, cerebral ischemia and strokes, and neuroinflammation [23-25]. CRMP2 phosphorylation causes microtubule dissociation and axonal outgrowth arrest [26]. Hyperphosphorylation of CRMP2 is an early event in the development of AD but not a common feature to other neurodegenerative diseases, perhaps suggesting that it could be an initially essential inducement and therapeutic target for AD [27-

Neuroprotection of ST2-104 in $A\beta_{25-35}$ -induced AD

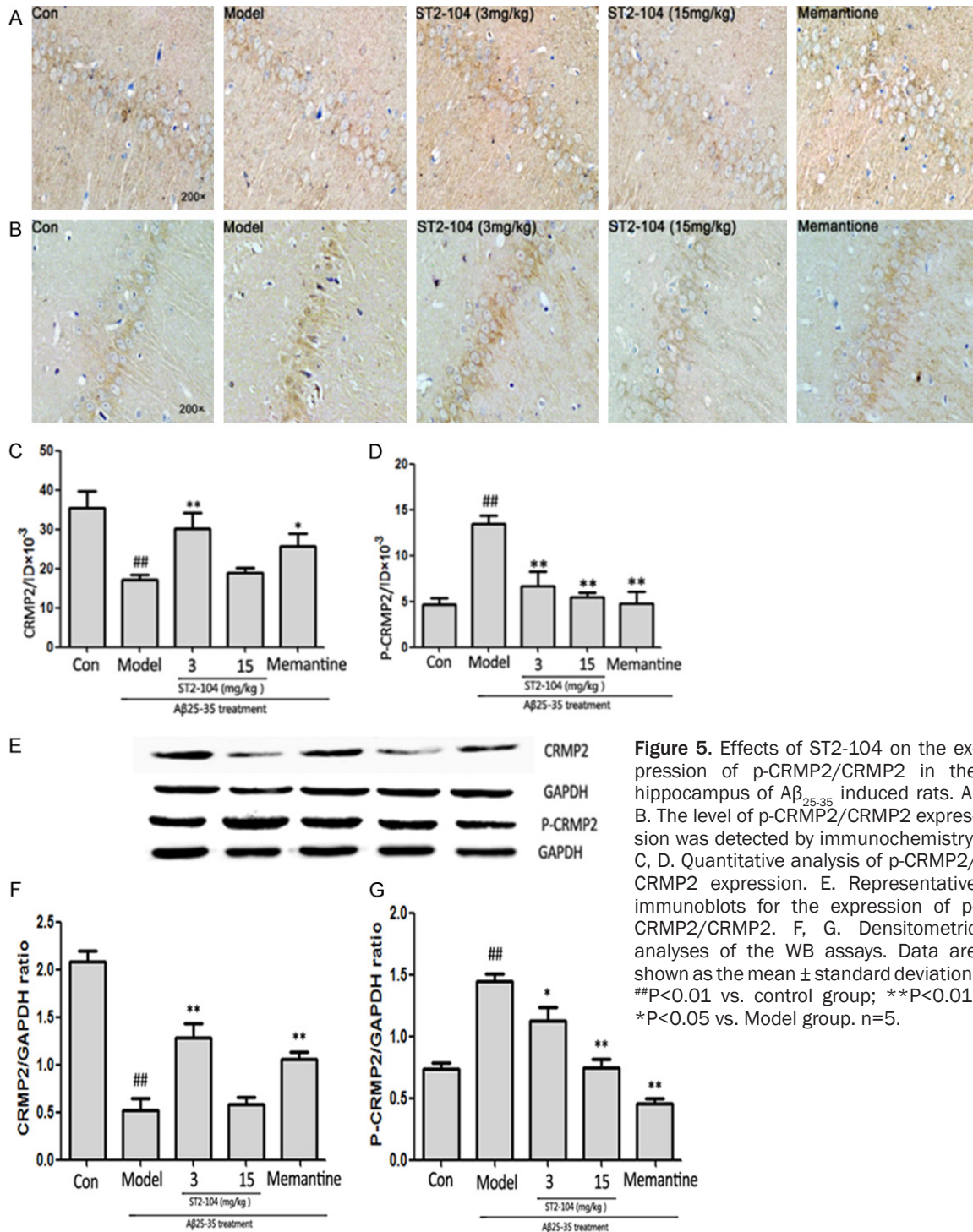


Figure 5. Effects of ST2-104 on the expression of p-CRMP2/CRMP2 in the hippocampus of $A\beta_{25-35}$ induced rats. A, B. The level of p-CRMP2/CRMP2 expression was detected by immunohistochemistry. C, D. Quantitative analysis of p-CRMP2/CRMP2 expression. E. Representative immunoblots for the expression of p-CRMP2/CRMP2. F, G. Densitometric analyses of the WB assays. Data are shown as the mean \pm standard deviation. ^{##} $P < 0.01$ vs. control group; ^{**} $P < 0.01$, ^{*} $P < 0.05$ vs. Model group. $n = 5$.

29]. This study demonstrated that the hyperphosphorylation of CRMP2 is an important factor in a $A\beta_{25-35}$ -induced AD rat model.

Small-molecule peptide aptamers targeting protein interactions have recently been proposed as potential therapeutic agents for many diseases. Specific sequence peptides derived

from endogenous proteins combine with congenetic sites of target proteins with high specificity and affinity, thus selectively regulating the function of the target proteins complex [30]. Unlike gene knockouts and RNA interference, which attenuate the expression of target proteins, peptide aptamers only regulate their relevant function, resulting in the functional inter-

Neuroprotection of ST2-104 in $A\beta_{25-35}$ -induced AD

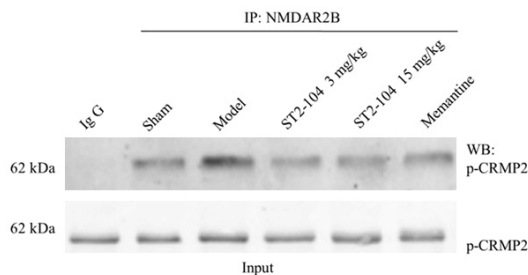


Figure 6. The effects of ST2-104 on the combination of NMDAR2B and p-CRMP2 in the hippocampus of $A\beta_{25-35}$ -induced rats. Coimmunoprecipitation was performed with normal IgG or anti-NMDAR2B antibody to capture the complexes, followed by Western blotting with anti-p-CRMP2 antibody. The input was directly immunoblotted with anti-p-CRMP2 antibody.

ference of signaling pathways [31, 32]. ST2-104 was conjugated CBD3 to the cell-penetrating peptide (CPP) R9 to structure a non-arginine (R9)-conjugated CBD3 (namely ST2-104) peptide, which has superior cell membrane permeability [33]. It has been shown that R9 is the most efficacious transduction domain protein in cells and that its toxicological effects are well tolerated by cells [34-36]. In the present study, ST2-104 remarkably improved spatial learning and memory in an $A\beta_{25-35}$ -induced AD rat model. Present findings also show that ST2-104 could attenuate expression of p-CRMP2 and increase expression of CRMP2 in the hippocampus.

Functional NMDARs are heterotetrameric complexes formed of two NMDAR1 and two NMDAR2 (NMDAR2A-D) subunits. They play a pivotal role in synaptic transmission plasticity for learning and memory and have been implicated in some neurological disorders [37]. NMDAR1 is continuously and steadily expressed, whereas expression of four NMDAR2 subunits (NMDAR2A-D) is temporally and spatially regulated in the brain [38]. The most studied NMDAR2B has been found in postsynaptic densities and the expression of NMDAR2B is constant and prominent within hippocampal CA1 [39, 40]. Overexpression of NMDAR2B in the forebrain has been previously shown to increase sensitivity to inflammatory pain [41]. Excessive calcium influx through overactive NMDARs can lead to excitotoxic neuronal death, thus suppression of overactive NMDARs has been shown to be neuroprotective [42]. Continuous activation of NMDARs has been recently implicated in AD related to synaptic dysfunction

[43]. $A\beta$ has been reported to trigger abnormal NMDARs-mediated Ca^{2+} influx, which may induce defective Ca^{2+} homeostasis, leading to excitotoxicity in neurons [44]. Additionally, $A\beta$ reduces surface expression of NMDAR subunit protein NMDAR1 [45]. $A\beta$ induces early neuronal dysfunction mediated by the excessive activation of NMDARs subunit protein NMDAR2B in hippocampal slices and primary neuronal cultures of mouse and rat [46]. Present findings demonstrate that $A\beta_{25-35}$ signally upregulated the total expression level of NMDAR2B protein, but not NMDAR1, in $A\beta_{25-35}$ -induced AD rats, suggesting that ST2-104 could attenuate expression of NMDAR2B.

Excessive Ca^{2+} influx through NMDARs, leading to activation of neurotoxic cascades, is thought to be a pivotal mediator of excitotoxicity because many antagonists of these receptors have neuroprotection in animal models of TBI and ischaemia-induced excitotoxicity [47-49]. However, the neuroprotection of NMDAR antagonists in many human trials has not been seen in animal models, though alarming side effects have been reported [50-53]. In contrast, memantine, a non-competitive NMDARs antagonist, is able to attenuate excitotoxicity and protects neurons in various models [54-56]. In clinical trials, memantine has shown significant promise in aspects of cognition for AD patients [57, 58]. The limit of NMDARs antagonists underscores the need for new small-molecule drugs that can protect neurons from excitotoxicity. Recent findings have suggested that NMDARs-interacting CRMP2 may be regarded as a novel neuroprotective target for various neurological disorders [12, 59]. Present findings also suggest that $A\beta_{25-35}$ treatment could strengthen the interaction of NMDAR2B and p-CRMP2, resulting in excessive NMDAR activity and neuronal excitotoxicity, whereas ST2-104 could attenuate the interaction of p-CRMP2 and NMDAR2B, decreasing concentrations of intracellular Ca^{2+} .

In conclusion, the present study reveals that ST2-104 derived from CRMP2 protein is a novel neuroprotective peptide for treatment of AD. Present findings show that ST2-104 may exert its neuroprotective effects by decreasing expression of NMDAR2B and p-CRMP2 and attenuating the interaction of p-CRMP2 and NMDAR2B, thus decreasing intracellular Ca^{2+} lev-

Neuroprotection of ST2-104 in $A\beta_{25-35}$ -induced AD

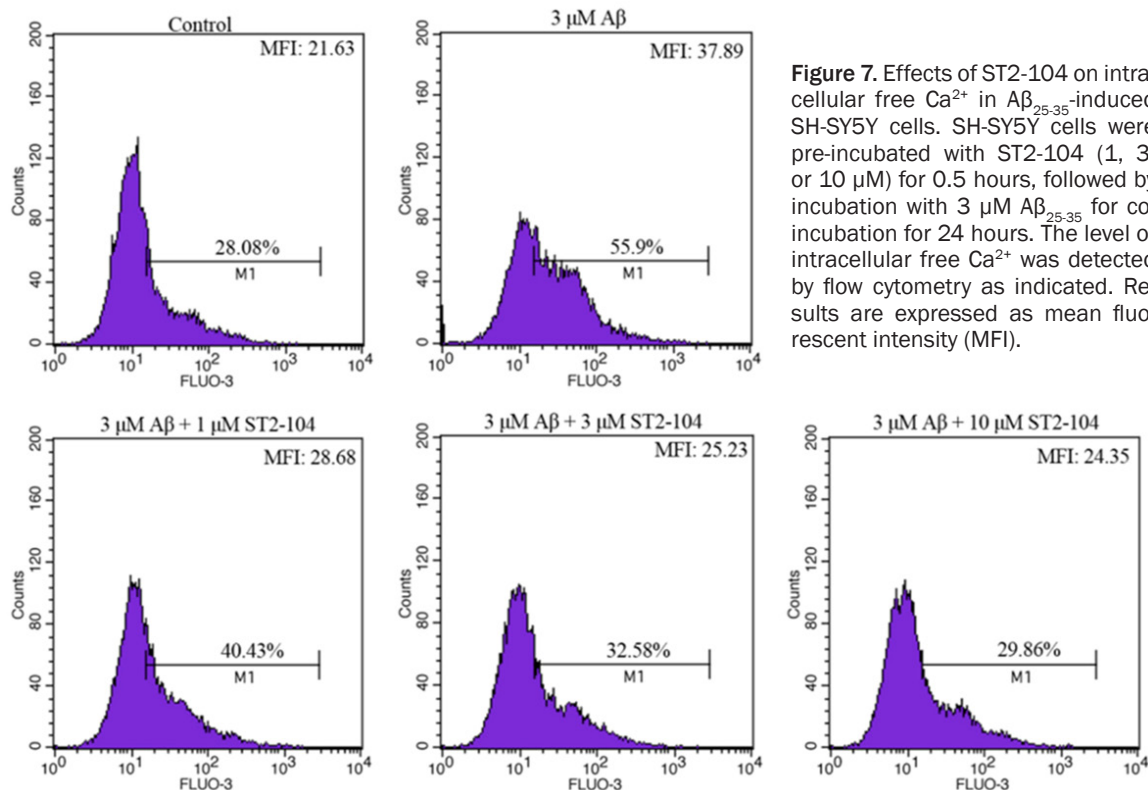


Figure 7. Effects of ST2-104 on intracellular free Ca^{2+} in $A\beta_{25-35}$ -induced SH-SY5Y cells. SH-SY5Y cells were pre-incubated with ST2-104 (1, 3, or 10 μ M) for 0.5 hours, followed by incubation with 3 μ M $A\beta_{25-35}$ for co-incubation for 24 hours. The level of intracellular free Ca^{2+} was detected by flow cytometry as indicated. Results are expressed as mean fluorescent intensity (MFI).

els. To further understand other possible biochemical mechanisms of ST2-104, future studies will determine whether ST2-104 regulates cell surface trafficking and endocytosis of NMDAR2B and NMDAR1 in an $A\beta_{25-35}$ -induced cell injury model. Importantly, the significant function of ST2-104 peptides indicates that this novel approach has the potential for translation into an effective therapeutic approach for AD.

Acknowledgements

This work was supported by the National Natural Science Foundation of China (grant nos. 81571231), Health and Family Planning Commission of Jilin Province (2015Z043), Department of Education Foundation of Jilin Province (JJKH20190102KJ), Department Science and Technology Foundation of Jilin Province (20190701058GH), and Talent Development Fund of Jilin Province (2014).

Disclosure of conflict of interest

None.

Address correspondence to: Li Sun, Department of Neurology and Neuroscience Center, The First

Hospital, Jilin University, Changchun 130021, Jilin, P. R. China. E-mail: huyang91@sohu.com

References

- [1] Blennow K, de Leon MJ and Zetterberg H. Alzheimer's disease. *Lancet* 2006; 368: 387-403.
- [2] Goedert M and Spillantini MG. A century of Alzheimer's disease. *Science* 2006; 314: 777-781.
- [3] Ubhi K and Masliah E. Alzheimer's disease: recent advances and future perspectives. *J Alzheimers Dis* 2013; 33 Suppl 1: S185-194.
- [4] Folch J, Petrov D, Ettcheto M, Abad S, Sanchez-Lopez E, Garcia ML, Olloquequi J, Beas-Zarate C, Auladell C and Camins A. Current research therapeutic strategies for Alzheimer's disease treatment. *Neural Plast* 2016; 2016: 8501693.
- [5] Paoletti P and Neyton J. NMDA receptor subunits: function and pharmacology. *Curr Opin Pharmacol* 2007; 7: 39-47.
- [6] Hansen KB, Furukawa H and Traynelis SF. Control of assembly and function of glutamate receptors by the amino-terminal domain. *Mol Pharmacol* 2010; 78: 535-549.
- [7] Zhang Y, Li P, Feng J and Wu M. Dysfunction of NMDA receptors in Alzheimer's disease. *Neurol Sci* 2016; 37: 1039-1047.
- [8] Birnbaum JH, Bali J, Rajendran L, Nitsch RM and Tackenberg C. Calcium flux-independent

- NMDA receptor activity is required for Abeta oligomer-induced synaptic loss. *Cell Death Dis* 2015; 6: e1791.
- [9] Danysz W and Parsons CG. Alzheimer's disease, beta-amyloid, glutamate, NMDA receptors and memantine—searching for the connections. *Br J Pharmacol* 2012; 167: 324-352.
- [10] Li S, Jin M, Koeglsperger T, Shepardson NE, Shankar GM and Selkoe DJ. Soluble Abeta oligomers inhibit long-term potentiation through a mechanism involving excessive activation of extrasynaptic NR2B-containing NMDA receptors. *J Neurosci* 2011; 31: 6627-6638.
- [11] Shankar GM, Bloodgood BL, Townsend M, Walsh DM, Selkoe DJ and Sabatini BL. Natural oligomers of the Alzheimer amyloid- β protein induce reversible synapse loss by modulating an NMDA-type glutamate receptor-dependent signaling pathway. *J Neurosci* 2007; 27: 2866-2875.
- [12] Al-Hallaq RA, Conrads TP, Veenstra TD and Wenthold RJ. NMDA Di-heteromeric receptor populations and associated proteins in rat hippocampus. *The Journal of Neuroscience* 2007; 27: 8334-8343.
- [13] Hooper C, Killick R and Lovestone S. The GSK3 hypothesis of Alzheimer's disease. *J Neurochem* 2008; 104: 1433-1439.
- [14] Morfini G, Szebenyi G, Brown H, Pant HC, Pignino G, DeBoer S, Beffert U and Brady ST. A novel CDK5-dependent pathway for regulating GSK3 activity and kinesin-driven motility in neurons. *EMBO J* 2004; 23: 2235-2245.
- [15] Brittain JM, Chen L, Wilson SM, Brustovetsky T, Gao X, Ashpole NM, Molosh AI, You H, Hudmon A, Shekhar A, White FA, Zamponi GW, Brustovetsky N, Chen J and Khanna R. Neuroprotection against traumatic brain injury by a peptide derived from the collapsin response mediator protein 2 (CRMP2). *J Biol Chem* 2011; 286: 37778-37792.
- [16] Brittain JM, Pan R, You H, Brustovetsky T, Brustovetsky N, Zamponi GW, Lee WH and Khanna R. Disruption of NMDAR-CRMP-2 signaling protects against focal cerebral ischemic damage in the rat middle cerebral artery occlusion model. *Channels* 2012; 6: 52-59.
- [17] Supnet C and Bezprozvanny I. The dysregulation of intracellular calcium in Alzheimer disease. *Cell Calcium* 2010; 47: 183-189.
- [18] Eisner DA, Venetucci LA and Trafford AW. Life, sudden death, and intracellular calcium. *Circ Res* 2006; 99: 223-224.
- [19] Stenmark P, Ogg D, Flodin S, Flores A, Kotenyova T, Nyman T, Nordlund P and Kursula P. The structure of human collapsin response mediator protein 2, a regulator of axonal growth. *J Neurochem* 2007; 101: 906-917.
- [20] Goshima Y, Nakamura F, Strittmatter P and Strittmatter SM. Collapsin-induced growth cone collapse mediated by an intracellular protein related to UNC-33. *Nature* 1995; 376: 509-514.
- [21] Kawano Y, Yoshimura T, Tsuboi D, Kawabata S, Kaneko-Kawano T, Shirataki H, Takenawa T and Kaibuchi K. CRMP-2 is involved in kinesin-1-dependent transport of the Sra-1/WAVE1 complex and axon formation. *Mol Cell Biol* 2005; 25: 9920-9935.
- [22] Fukata Y, Itoh TJ, Kimura T, Menager C, Nishimura T, Shiromizu T, Watanabe H, Inagaki N, Iwamatsu A, Hotani H and Kaibuchi K. CRMP-2 binds to tubulin heterodimers to promote microtubule assembly. *Nat Cell Biol* 2002; 4: 583-591.
- [23] Schmidt EF and Strittmatter SM. The CRMP family of proteins and their role in Sema3A signaling. *Adv Exp Med Biol* 2007; 600: 1-11.
- [24] Yoshida H, Watanabe A and Ihara Y. Collapsin response mediator protein-2 is associated with neurofibrillary tangles in Alzheimer's disease. *J Biol Chem* 1998; 273: 9761-9768.
- [25] Chen A, Liao WP, Lu Q, Wong WS and Wong PT. Upregulation of dihydropyrimidinase-related protein 2, spectrin alpha II chain, heat shock cognate protein 70 pseudogene 1 and tropomodulin 2 after focal cerebral ischemia in rats—a proteomics approach. *Neurochem Int* 2007; 50: 1078-1086.
- [26] Arimura N, Menager C, Kawano Y, Yoshimura T, Kawabata S, Hattori A, Fukata Y, Amano M, Goshima Y, Inagaki M, Morone N, Usukura J and Kaibuchi K. Phosphorylation by Rho kinase regulates CRMP-2 activity in growth cones. *Mol Cell Biol* 2005; 25: 9973-9984.
- [27] Cole AR, Noble W, van Aalten L, Plattner F, Meimaridou R, Hogan D, Taylor M, LaFrancois J, Gunn-Moore F, Verkhatsky A, Oddo S, LaFerla F, Giese KP, Dineley KT, Duff K, Richardson JC, Yan SD, Hanger DP, Allan SM and Sutherland C. Collapsin response mediator protein-2 hyperphosphorylation is an early event in Alzheimer's disease progression. *J Neurochem* 2007; 103: 1132-1144.
- [28] Williamson R, van Aalten L, Mann DM, Platt B, Plattner F, Bedford L, Mayer J, Howlett D, Usardi A, Sutherland C and Cole AR. CRMP2 hyperphosphorylation is characteristic of Alzheimer's disease and not a feature common to other neurodegenerative diseases. *J Alzheimers Dis* 2011; 27: 615-625.
- [29] Hensley K, Venkova K, Christov A, Gunning W and Park J. Collapsin response mediator protein-2: an emerging pathologic feature and therapeutic target for neurodegenerative diseases. *Mol Neurobiol* 2011; 43: 180-191.

Neuroprotection of ST2-104 in $A\beta_{25-35}$ -induced AD

- [30] Fischer G, Pan B, Vilceanu D, Hogan QH and Yu H. Sustained relief of neuropathic pain by AAV-targeted expression of CBD3 peptide in rat dorsal root ganglion. *Gene Ther* 2014; 21: 44-51.
- [31] Colombo M, Mizzotti C, Masiero S, Kater MM and Pesaresi P. Peptide aptamers: the versatile role of specific protein function inhibitors in plant biotechnology. *J Integr Plant Biol* 2015; 57: 892-901.
- [32] Sergey R, David SB and Alexander S. Peptide aptamers: development and applications. *Current Topics in Medicinal Chemistry* 2015; 15: 1082-1101.
- [33] Wender PA, Mitchell DJ, Pattabiraman K, Pelkey ET, Steinman L and Rothbard JB. The design, synthesis, and evaluation of molecules that enable or enhance cellular uptake: peptoid molecular transporters. *Proc Natl Acad Sci U S A* 2000; 97: 13003-13008.
- [34] Mitchell DJ, Steinman L, Kim DT, Fathman CG and Rothbard JB. Polyarginine enters cells more efficiently than other polycationic homopolymers. *J Pept Res* 2000; 56: 318-325.
- [35] Tunnemann G, Ter-Avetisyan G, Martin RM, Stockl M, Herrmann A and Cardoso MC. Live-cell analysis of cell penetration ability and toxicity of oligo-arginines. *J Pept Sci* 2008; 14: 469-476.
- [36] Duchardt F, Fotin-Mleczek M, Schwarz H, Fischer R and Brock R. A comprehensive model for the cellular uptake of cationic cell-penetrating peptides. *Traffic* 2007; 8: 848-866.
- [37] Tovar KR, McGinley MJ and Westbrook GL. Triheteromeric NMDA receptors at hippocampal synapses. *J Neurosci* 2013; 33: 9150-9160.
- [38] Monyer H, Burnashev N, Laurie DJ, Sakmann B and Seeburg PH. Developmental and regional expression in the rat brain and functional properties of four NMDA receptors. *Neuron* 1994; 12: 529-540.
- [39] Goebel-Goody SM, Davies KD, Alvestad Linger RM, Freund RK and Browning MD. Phosphoregulation of synaptic and extrasynaptic N-methyl-D-aspartate receptors in adult hippocampal slices. *Neuroscience* 2009; 158: 1446-1459.
- [40] Zhou Y, Takahashi E, Li W, Halt A, Wiltgen B, Ehninger D, Li GD, Hell JW, Kennedy MB and Silva AJ. Interactions between the NR2B receptor and CaMKII modulate synaptic plasticity and spatial learning. *J Neurosci* 2007; 27: 13843-13853.
- [41] Wei F, Wang GD, Kerchner GA, Kim SJ, Xu HM, Chen ZF and Zhuo M. Genetic enhancement of inflammatory pain by forebrain NR2B overexpression. *Nat Neurosci* 2001; 4: 164-169.
- [42] Lee JM, Zipfel GJ and Choi DW. The changing landscape of ischaemic brain injury mechanisms. *Nature* 1999; 399: A7-A14.
- [43] Mota SI, Ferreira IL and Rego AC. Dysfunctional synapse in Alzheimer's disease - a focus on NMDA receptors. *Neuropharmacology* 2014; 76 Pt A: 16-26.
- [44] Bezprozvanny I and Mattson MP. Neuronal calcium mishandling and the pathogenesis of Alzheimer's disease. *Trends Neurosci* 2008; 31: 454-463.
- [45] Hoey SE, Williams RJ and Perkinson MS. Synaptic NMDA receptor activation stimulates alpha-secretase amyloid precursor protein processing and inhibits amyloid-beta production. *J Neurosci* 2009; 29: 4442-4460.
- [46] Ronicke R, Mikhaylova M, Ronicke S, Meinhardt J, Schroder UH, Fandrich M, Reiser G, Kreuz MR and Reymann KG. Early neuronal dysfunction by amyloid beta oligomers depends on activation of NR2B-containing NMDA receptors. *Neurobiol Aging* 2011; 32: 2219-2228.
- [47] Mattson MP. Excitotoxic and excitoprotective mechanisms. *NeuroMolecular Medicine* 2003; 3: 65-94.
- [48] Olney JW, Wozniak DF and Farber NB. Excitotoxic neurodegeneration in Alzheimer disease: new hypothesis and new therapeutic strategies. *Archives of Neurology* 1997; 54: 1234-1240.
- [49] Bano D, Young KW, Guerin CJ, Lefevre R, Rothwell NJ, Naldini L, Rizzuto R, Carafoli E and Nicotera P. Cleavage of the plasma membrane Na^+/Ca^{2+} exchanger in excitotoxicity. *Cell* 2005; 120: 275-285.
- [50] Farooqui AA, Ong WY and Horrocks LA. Inhibitors of brain phospholipase A2 activity: their neuropharmacological effects and therapeutic importance for the treatment of neurologic disorders. *Pharmacol Rev* 2006; 58: 591-620.
- [51] Brustovetsky T, Bolshakov A and Brustovetsky N. Calcineurin activation and Na^+/Ca^{2+} exchanger degradation occur downstream of calcium deregulation in hippocampal neurons exposed to excitotoxic glutamate. *J Neurosci Res* 2010; 88: 1317-1328.
- [52] Manev H, Favaron M, Guidotti A and Costa E. Delayed increase of Ca^{2+} influx elicited by glutamate: role in neuronal death. *Mol Pharmacol* 1989; 36: 106-112.
- [53] Thayer SA and Miller RJ. Regulation of the intracellular free calcium concentration in single rat dorsal root ganglion neurones in vitro. *J Physiol* 1990; 425: 85-115.
- [54] Song MS, Rauw G, Baker GB and Kar S. Memantine protects rat cortical cultured neurons

Neuroprotection of ST2-104 in $A\beta_{25-35}$ -induced AD

- against β -amyloid-induced toxicity by attenuating tau phosphorylation. *Eur J Neurosci* 2008; 28: 1989-2002.
- [55] Budd SL and Nicholls DG. Mitochondria, calcium regulation, and acute glutamate excitotoxicity in cultured cerebellar granule cells. *J Neurochem* 1996; 67: 2282-2291.
- [56] Tymianski M, Charlton M, Carlen P and Tator C. Source specificity of early calcium neurotoxicity in cultured embryonic spinal neurons. *J Neurosci* 1993; 13: 2085-2104.
- [57] Parsons CG, Danysz W and Quack G. Memantine is a clinically well tolerated N-methyl-d-aspartate (NMDA) receptor antagonist-a review of preclinical data. *Neuropharmacology* 1999; 38: 735-767.
- [58] Wilkinson D. A review of the effects of memantine on clinical progression in Alzheimer's disease. *Int J Geriatr Psychiatry* 2012; 27: 769-776.
- [59] Bretin S, Rogemond V, Marin P, Maus M, Torrens Y, Honnorat J, Glowinski J, Premont J and Gauchy C. Calpain product of WT-CRMP2 reduces the amount of surface NR2B NMDA receptor subunit. *J Neurochem* 2006; 98: 1252-1265.